



Fermi National Accelerator Laboratory

FERMILAB-Pub-89/169

**Cerium Fluoride:
A Scintillator for High-Rate Applications ***

D. F. Anderson

*Fermi National Accelerator Laboratory
P.O. Box 500, Batavia, Illinois 60510*

August 1989

* Submitted to Nucl. Instrum. Methods A.



Cerium Fluoride: A Scintillator For High-Rate Applications

D.F. Anderson
Particle Detector Group
Fermi National Accelerator Laboratory
Batavia IL 60510 U.S.A.

(Submitted to Nuclear Instruments and Methods A)

Abstract

Measurements of the temperature dependence, over a 400°C range, of the scintillation yield of CeF₃ are presented. A separation of the fast (≈5 ns) and slow (30 ns) components is made at room temperature and at liquid nitrogen temperature. It is estimated that the fast component increases from 33% to 60% when the crystal is cooled. The use of inexpensive starting material reduces the slow component with little or no loss of fast component. Applications for CeF₃, primarily high-rate PET, are also discussed.

1. Introduction

In both the fields of high-energy physics and nuclear medicine, there has been a constant search for new scintillators. Recently, this effort has produced the new scintillator cerium fluoride, CeF_3 [1,2]. Although the growing of large crystals of CeF_3 is still under development in a collaboration between Fermilab and Optovac, Inc.,(North Brookfield, MA), it is gaining interest as a possible fast scintillator in the field of positron emission tomography, PET. To put the scintillators available for this application in better perspective, Table 1 lists the properties of the various inorganic scintillators. The major problems of the various scintillators for use in PET are also given. The parameter of light yield was not considered.

At present, the two major scintillators used for PET are BGO and BaF_2 . Because of its high density and high atomic number, BGO is the workhorse of high-resolution, non-time-of-flight PET. It also has the best total absorption efficiency of any of the crystals used. Its one drawback is that its relatively long scintillation decay constant of 300 ns limits its usefulness at high rates.

For time-of-flight PET, BaF_2 is the crystal of choice. About 20% of its light is in the "fast component" with a decay constant of only about 0.8 ns. This is the fastest decay constant known for an inorganic scintillator. For high-rate applications the "slow component," with a decay constant of 620 ns, has been removed electronically with some success. The major drawback of BaF_2 is that the fast component has its peak emission at 225 nm; thus, quartz photomultipliers (PMT) must be used. This greatly increases the cost of a PET camera, which has substantially limited the use of time-of-flight PET.

As can be seen from Table 1, CeF_3 falls somewhere between BGO and BaF_2 in many aspects such as density, absorption length at 511 keV, and index of refraction with values of 6.16 g/cm³, 1.9 cm, and 1.68, respectively. Like BaF_2 , it has two (possibly three) emission components with decay times of ≈ 5 ns and 30 ns. Although CeF_3 is not as fast as the fast component of BaF_2 , its slow component is a factor of 20 faster than the slow component of BaF_2 and a factor of 10 faster than BGO. The amount of light produced by the CeF_3 is estimated to be about 50% that of BGO and on the order of that of the fast component of BaF_2 . A timing resolution for a single CeF_3 PET crystal of 0.56 ns has also been achieved[1].

Figure 1 shows the emission spectrum and transmission as a function of wavelength of CeF_3 at room temperature. The peak emission is at about 340 nm, but as will be shown below, there are in fact two components in this emission. In comparing the light output with a quartz and a glass PMT, the quartz PMT gave about a 15% larger signal. If there is

a reason to detect this small addition in light output, a UV-glass PMT can be used, which adds little to the cost.

In this work we will present the scintillation intensity of CeF_3 as a function of temperature over a range of almost 400°C , as well as the relative intensities of the fast and slow components at room temperature and at liquid nitrogen, LN_2 , temperature. We will also discuss the results of adding dopants to produce clearer crystals and the characteristics of crystals made with inexpensive starting material.

2. Experimental Technique

For the measurements of both the total light output and the scintillation decay spectra of CeF_3 as a function of temperature, the delayed coincidence method was used[10] with a 1-cm cube that was doped with 0.5% BaF_2 (see section 6). The sample was placed in either a small oven with a quartz window, or in a temperature-controlled cryostat, also with a quartz window. A ^{22}Na radioactive source of 511-keV annihilation photons was used. A BaF_2 crystal coupled to a quartz PMT (Hamamatsu R2059) provided the start signal to a LeCroy model 3001 qVt operated in the time mode, while a similar quartz PMT viewing the sample from some distance through the quartz window provided the stop signal. Since the stop PMT saw on the average much less than one photon per start, the time spectrum built up gives a true representation of the scintillation decay shape.

This technique also worked well for determining the relative light yields. Since both the oven and the cryostat prevented good optical coupling to the PMT, the pulse height from an x-ray line could not be measured. We took the relative light yield to be proportional to the number of stops per start. This assumption has been confirmed by reproduction of the shape of the high-temperature part of our curve with another technique[11].

3. Absolute Light Output at Room Temperature

The measurement of the absolute light output of a scintillator is difficult because it depends on the quality of the surfaces, the reflective coating, optical couplings, and the quantum efficiency of the PMT. Measurements have been made comparing CeF_3 to a BGO crystal of the same dimensions[1,2]. The results place an estimate on the light output of CeF_3 at about 50% that of BGO. Taking the value of BGO to be 7-10% that of $\text{NaI}(\text{Tl})$, this puts limits on the light output of CeF_3 at 3-5% of $\text{NaI}(\text{Tl})$.

Figure 2 shows the pulse-height spectrum for 511-keV gamma rays. The energy resolution is 19.3% FWHM. By comparing the pulse height of the crystal to the signal using an LED whose intensity has been reduced to make the resolution light limited, we

find that the average number of photoelectrons in the peak is 205. (A conservative correction was made for the contribution to the resolution of the LED by the finite gain of the first dynode[12].) If one assumes a quantum efficiency of 20-25% for the PMT, and neglects other sources of loss, this implies $1.6\text{-}2.0 \times 10^3$ photons per MeV are produced in the crystal. This is 4-5% of the number given for NaI(Tl) in the literature[13].

4. Relative Light Output as a Function of Temperature

It was noted earlier[1] that when CeF_3 is cooled, a second peak develops in the emission spectrum. This is seen in Fig. 3 which shows the emission spectrum for CeF_3 at 20°C as well as for -30°C , -102°C , and -168°C . In the same work we showed that this second peak with its maximum at 310 nm is associated with the fast component in CeF_3 .

The light output of CeF_3 as a function of temperature over a range of almost 400°C is shown in Fig. 4. Since half the data was taken with the crystal in an oven and half with a cryostat, the two sets of data had to be normalized at their overlap at room temperature. Thus, the light output was normalized to a value of 1 at 20°C .

If one compares the temperature response of CeF_3 given in Fig. 4 to the response of Na(Tl) and doped CsI[14], there is a significant difference when cooled. The light output of Na(Tl) and doped CsI decrease significantly as they are cooled. The light output of CeF_3 first decreases slightly as it is cooled, but starts to increase again at temperatures below about 0°C . This response is similar to that of cooled BGO[4] and also pure CsI[15] whose light output increases monotonically down to -150°C before turning over.

5. Decay Constants

The scintillation intensity as a function of time (decay curve) for CeF_3 , taken with a quartz PMT at room temperature, is shown in Fig. 5. It is obvious that there is more than one decay constant. A simple fit gives a decay constant of 26.9 ns. To separate the components of the decay spectrum, a glass filter (with a cutoff at about 330 nm), was placed over the quartz PMT face. This filter removes much of the fast component[1] (somewhat more than would be removed by a glass PMT). We normalized this decay curve to the quartz decay curve at long scintillation times and subtracted it from the quartz decay curve. Since the spectrum that remains corresponds to the bluest light and therefore is associated with the short decay component, we have thus generated a decay curve with only the fast component. We then re-normalized this curve such that it equals the apparent residual fast component in the spectrum taken with the glass filter and subtracted it from the glass-filter curve. The results of this subtraction, which yields the room-temperature slow

component, is shown in Fig. 6. One can see that the curve is now well fit by a single decay constant of 30.3 ns.

The room-temperature fast component is the difference Fig. 6 from Fig. 5, and is shown in Fig. 7. This curve can be fitted with two decay constants of 5.0 ns and 8.7 ns. The longer decay constant may represent a third component to the decay, or it may be an artifact of the technique used to separate the decay constants. Figure 8 shows the fast and slow components on a linear scale. At room temperature, it appears that about 33% of the scintillation is in the fast component.

An analysis similar to the above was performed on the decay curves at LN₂ temperature. Figure 9 shows the decay curve taken with a quartz PMT. By comparison with Fig. 5, one sees that there is a larger fraction of the light in the fast component. The simple fit to the decay is now 25.5 ns. The extracted slow component curve at LN₂ temperature is shown in fig. 10, which is fit by a single decay constant of 35.8 ns. This is longer than at room temperature. Figure 11 shows the fast component, which is again fitted by two decay constants of 5.5 ns and 10.5 ns. These values are also a little longer than the room temperature values. Figure 12 shows the separated fast and slow components at LN₂ temperatures. The fast component is now 60% of the emission. As can be seen from Fig.4, the total emission is 10% larger than at room temperature. Thus, at LN₂ temperatures, there are a factor of two more photons in the fast component.

6. Divalent Dopants and Starting Materials.

As stated above, the growing of CeF₃ is still in the development stage. Two of the main objectives in our work in growing CeF₃ have been to produce high-quality scintillators both reliably and at minimum cost. The addition of the divalent additives has made a substantial contribution to realizing the first objective. Earlier efforts at adding dopants have not been successful in producing material with better performance than is achieved with clear CeF₃[1]. Divalent fluorides (i.e., CaF₂, SrF₂, and BaF₂), added on the <2% level, have proven useful for the growing of clear material. There is still a great deal of work to be done to quantify this effect, but crystals grown with the addition of a divalent fluoride have consistently had better transmissions and higher light outputs than other crystals in the same growth. From measurements and theory we are lead to believe that the best dopant is CaF₂, because it has a similar lattice size to CeF₃[16]. The amount of additive needed seems to be dependent upon the quality of the starting material.

In the search for cost reduction we have gone as far as using starting materials that were only 99% pure CeF₃. The remaining 1% consisted primarily of other rare-earth fluorides (DyF₃, EuF₃, YrF₃, GdF₃, and SnF₃)[17]. The term "rare earth" is a misnomer,

since they are not rare. Their expense comes largely from the difficulty in their purification. If low-quality material can be used to make good scintillators, there would be a substantial reduction in production costs.

With the addition of a small amount of divalent fluoride to the 99% pure starting material, good transmissions were achieved. Figure 13 shows the transmission of one sample doped with 0.5% CaF_2 . The sharp cutoff at short wavelengths is typical for material with a divalent dopant. A second sample doped with 0.5% BaF_2 had an almost identical transmission. Figure 13 also shows the emission spectra (excited with 254-nm uv light) of the two samples doped with CaF_2 and BaF_2 . The BaF_2 doped material has an emission spectrum that differs significantly from that of pure CeF_3 , and there is also a lesser difference for the CaF_2 doped material.

Both samples of CeF_3 showed a reduction in light output about 37% less than a sample made of high purity starting material. Figure 14 shows the decay curve of the BaF_2 -doped sample taken with a quartz PMT at room temperature. By comparing this curve with Fig. 5, one can see that there is a much higher fraction of the signal in the fast component. When the glass filter was used, the decay curve in fig. 15 was obtained. By comparison with fig. 6, which is similar to the raw data for the high-purity crystal with the glass filter, one can see that there is much more of the fast component remaining. Thus, the fast component is shifted towards the longer wavelengths. The decay curves for the CaF_2 doped material was almost indistinguishable from those taken with the BaF_2 -doped material.

The results of our analysis of the decay spectrum of the 99% material are consistent with the assumption that all of the 37% reduction in light output comes from the slow component. By combining the fast component of the high-purity CeF_3 (Fig. 7) with 45% of its slow component (Fig. 6) the resulting decay spectrum was almost identical to the decay spectra for the 99% material doped with either CaF_2 or BaF_2 . These results are similar to the results with BaF_2 [18,19] where the addition of a small concentration of dopant such as Tm or La causes a substantial reduction in the slow component while having little effect on the fast component.

7. Discussion

CeF_3 has good gamma-ray stopping power and good mechanical properties. Its scintillation yield has a good temperature dependence from about -200°C to $+100^\circ\text{C}$, and there are also indications that it is radiation hard[1]. Its biggest advantage over the other scintillators is that it is very fast, with decay constants of ≈ 5 ns and 30 ns, without the very long component of several hundred nanosecond that some of the other scintillators

have. This makes it the fastest high-Z, inorganic scintillator available. (To our knowledge, CsF is not commercially available at present because of the difficulties in its growth.) CeF₃ is most useful where ever high-energy spectroscopy needs to be done at high rates. The most obvious application to come to mind is that of high-rate PET, but there are applications in nuclear physics and in radiation monitoring. It is useful wherever there is a very high background, and it may find a use in such an application as the detection of the 10.8-MeV nitrogen gamma line for explosives detection.

References

1. D.F. Anderson, IEEE Trans. Nucl. Sci. NS-36 (1989) 137.
2. W.W. Moses and S.E. Derenzo, IEEE Trans. Nucl. Sci. NS-36 (1989) 173.
3. C.L. Woody and D.F. Anderson, Nucl. Instr. and Methods, A265 (1988) 291.
4. Harshaw/Filtrol (now Engelhart Corp.), "Scintillation Detectors: A Reference Guide"
5. H. Kobayashi et. al., "Pure CsI; New Fast Scintillator for γ -Detectors", KUNS-900, November 1987.
6. S. Kubota et. al., Nucl. Instr. and Methods, A268 (1988) 275.
7. S.Sakuragi et. al., "Development and Applications of Pure CsI Scintillator with 10 ns Decay Time at Room Temperature," presented at the 2nd Technical Meeting of KEK on "Radiation Detectors and Dosimetry," Jan.19, 20, 1987, at KEK.
8. Particle Data Group, "Review of Particle Properties," Phys. Lett. 170B (1986) 1.
9. T. Kazumasa and T. Fukazawa, Appl. Phys. Lett.42 #1 (1983) 43.
10. L.M. Bollinger and G.E. Thomas, Nucl. Instr. and Methods 32 (1961) 1044.
11. C.L. Melcher, Schlumberger-Doll Research, private communication.
12. RCA Photomultiplier Handbook
13. R. Allemand et. al., "New Developments in Fast Timing With BaF₂ Scintillator", LETI/MCTE/82-245.
14. R.L. Heath et.al., Nucl. Instr. and Methods 162 (1979) 431.
15. This author, data to be published elsewhere.

16. M.J. Weber, Lawrence Livermore National Laboratory, private communication.
17. R. Sparrow, Optovac, Inc., private communication.
18. P. Schotanus et. al., IEEE Trans. Nucl. Sci. NS-34 (1987) 272.
19. C.L. Woody, P.W. Levy, and J.A. Kierstead, IEEE Trans. Nucl. Sci. NS-36 (1989) 536.

Table 1.

Properties of various inorganic scintillators

	CeF ₃ ^[1]	BaF ₂ ^[3]	BGO ^[4]	CsF ^[4]	CsI ^[5-7]	CsI(Tl) ^[4,7]	NaI(Tl) ^[4,8]	GSO ^[9]
Density	6.16	4.9	7.13	4.64	4.53	4.53	3.67	6.71
Absorption length (1/e in cm, at 511 keV)	1.9	2.3	1.1	2.3	1.8	1.8	2.9	
Radiation length (cm)	1.7	2.1	1.1	2.0	1.86	1.86	2.6	
Decay constant -short (n sec) -long	≈5 30	0.6 620	300	2.8 4.4	≈10, 36 >1000	>1000	230 150 ms	60
Peak emission -short (nm) -long	310 340	220 310	480	390	300 >400	550	415	430
Index of refraction at peak emission	1.68	1.56	2.15	1.48	1.8	1.8	1.85	1.9
Light yield [NaI(Tl)≡100]	4-5	5 16	7-10	6	3.7	85	100	20
Hygroscopic	No	Slight	No	Very	Slight	Slight	Yes	No
Problems for PET		q PMT Slow comp.	Slow	Hyg. Cost	uv gl. PMT Slow comp.	Slow	Slow	Cost

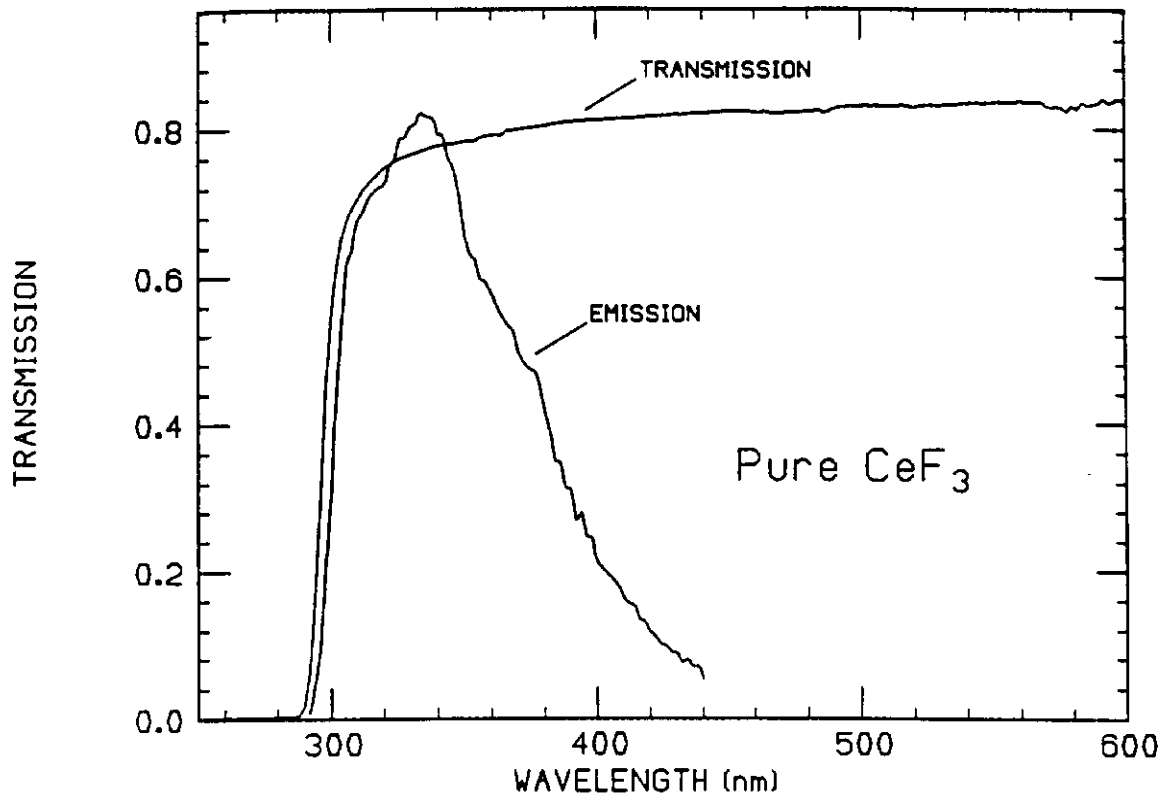


Figure 1 Emission spectrum and transmission as a function of wavelength of CeF_3 at room temperature.

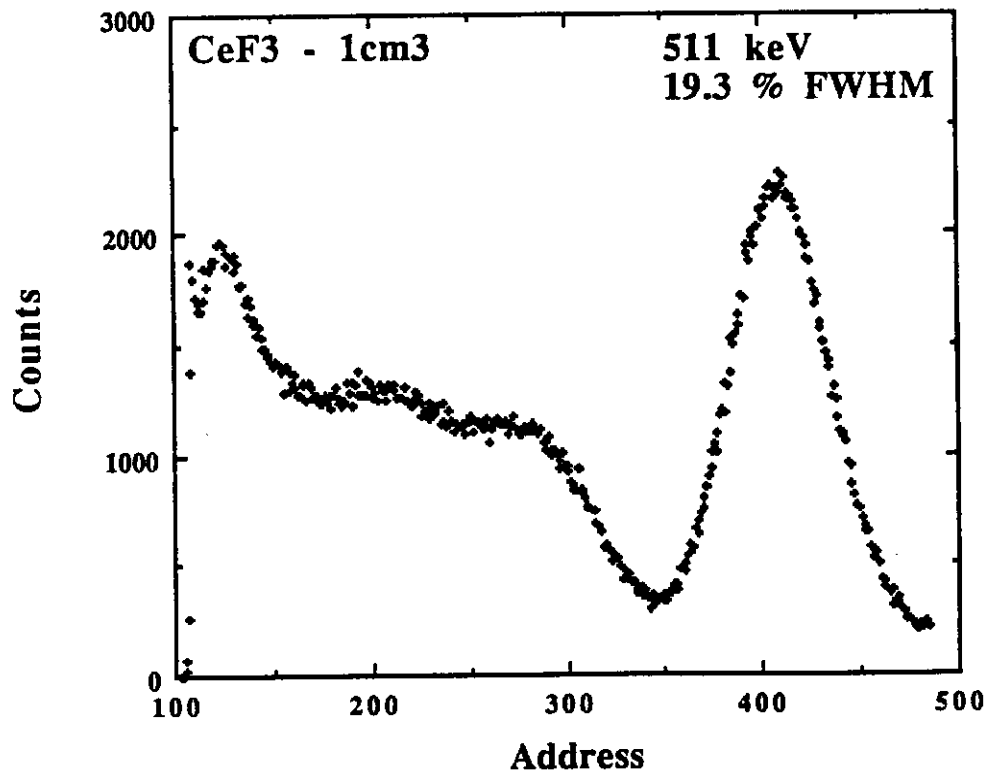


Figure 2 Pulse-height spectrum for 511-keV gamma rays.

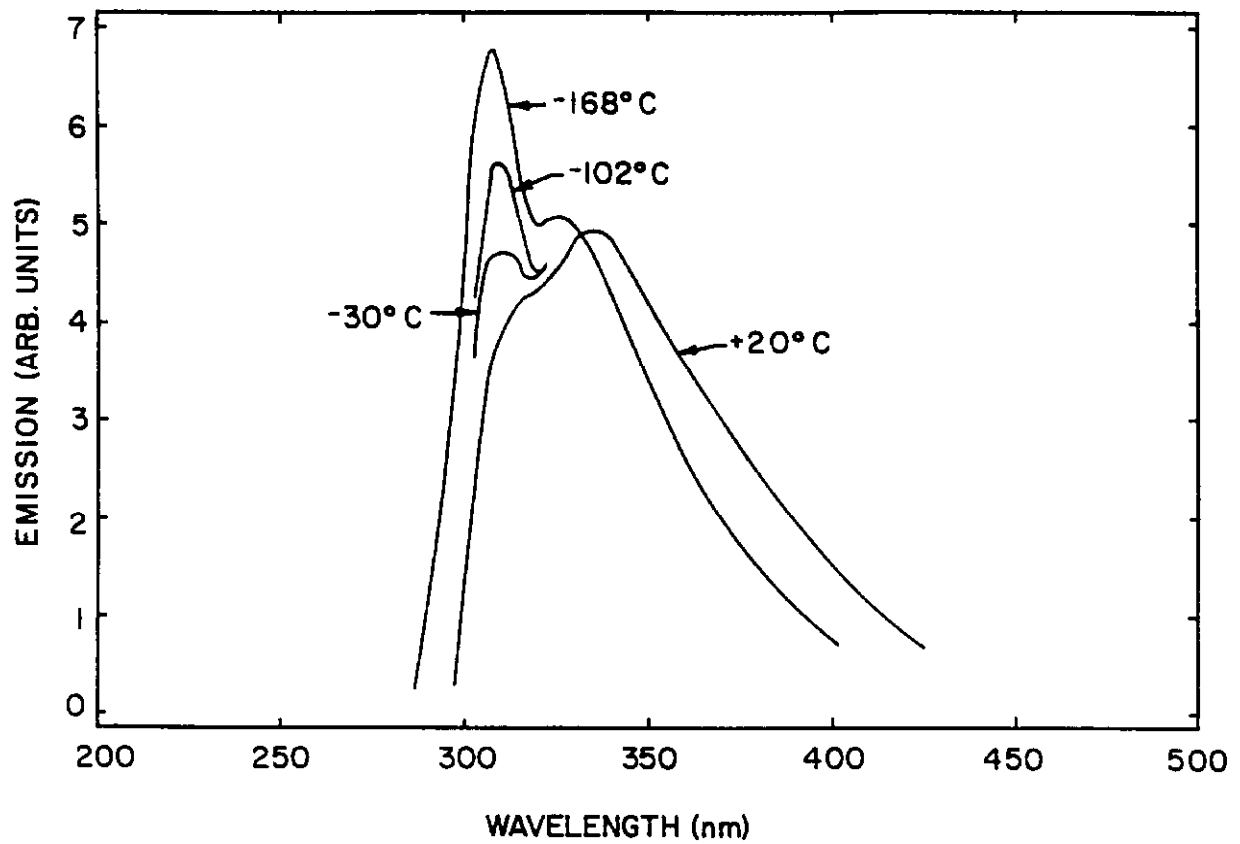


Figure 3 Emission spectrum of CeF_3 at +20, -30, -102, and -168°C

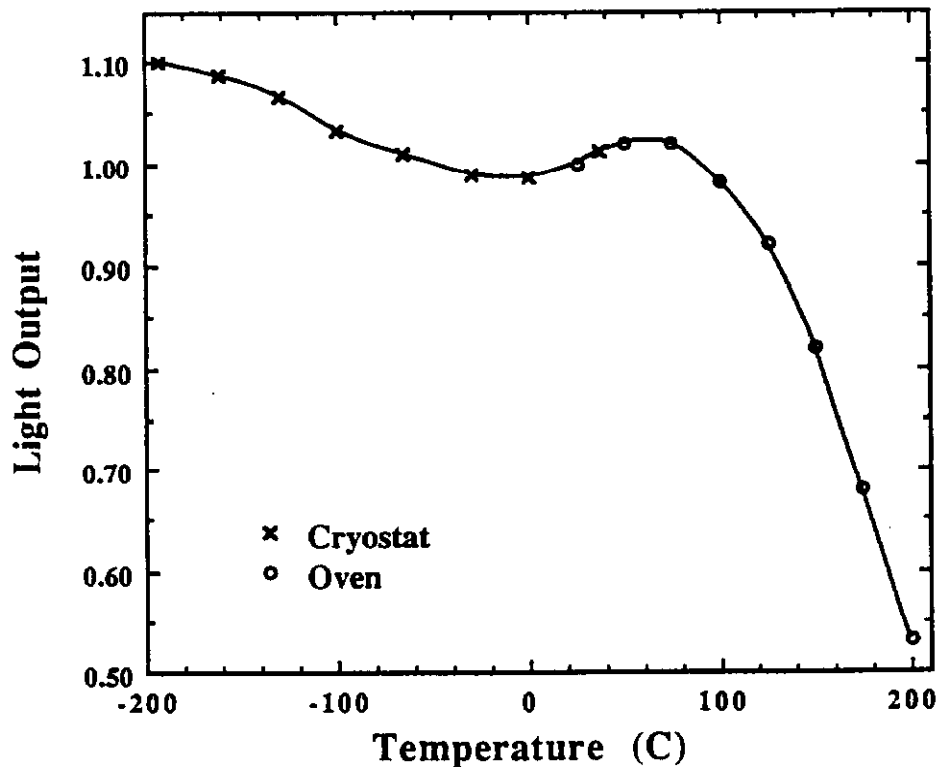


Figure 4 Light output of CeF_3 as a function of temperature.

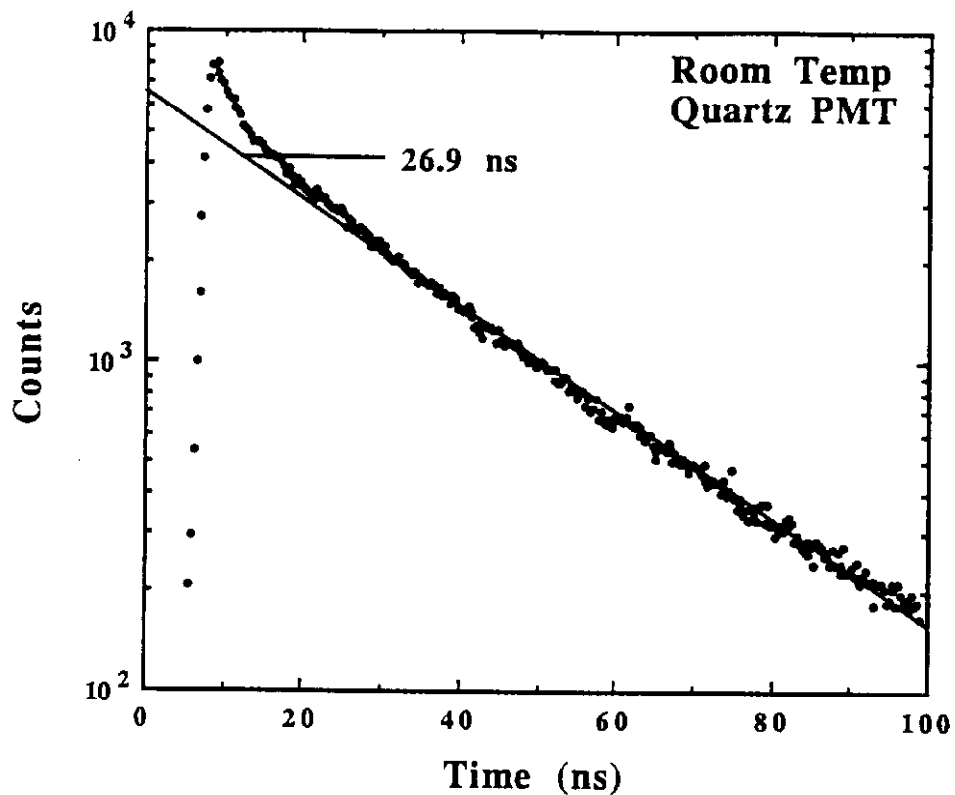


Figure 5 Scintillation decay curve with a quartz PMT at room temperature .

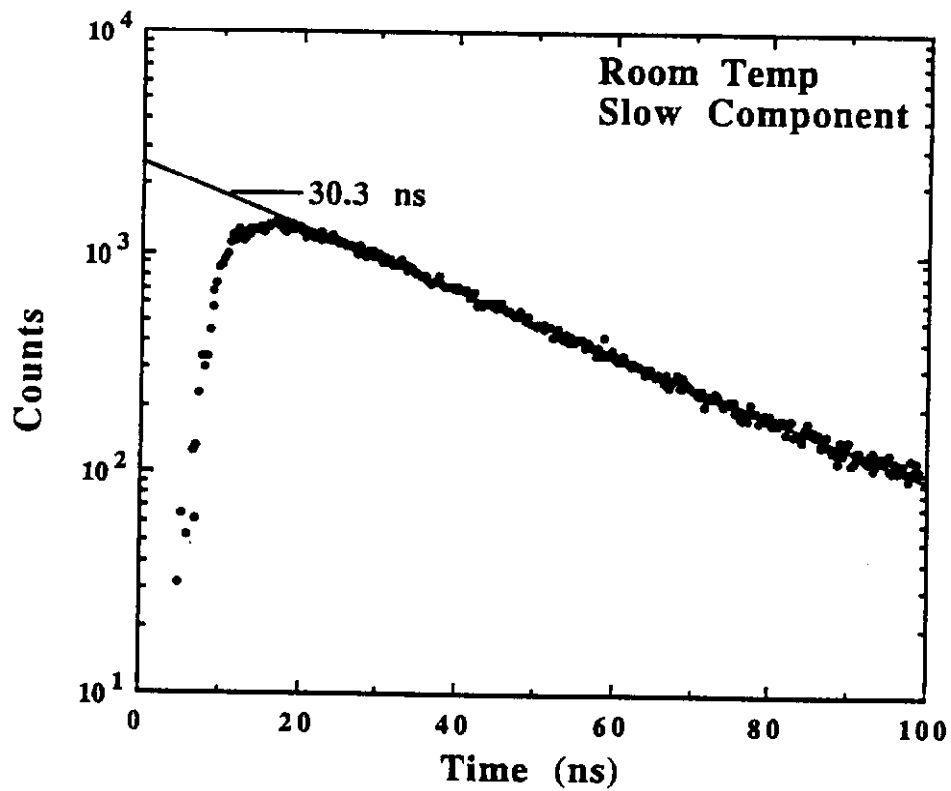


Figure 6 Scintillation decay curve of slow component at room temperature.

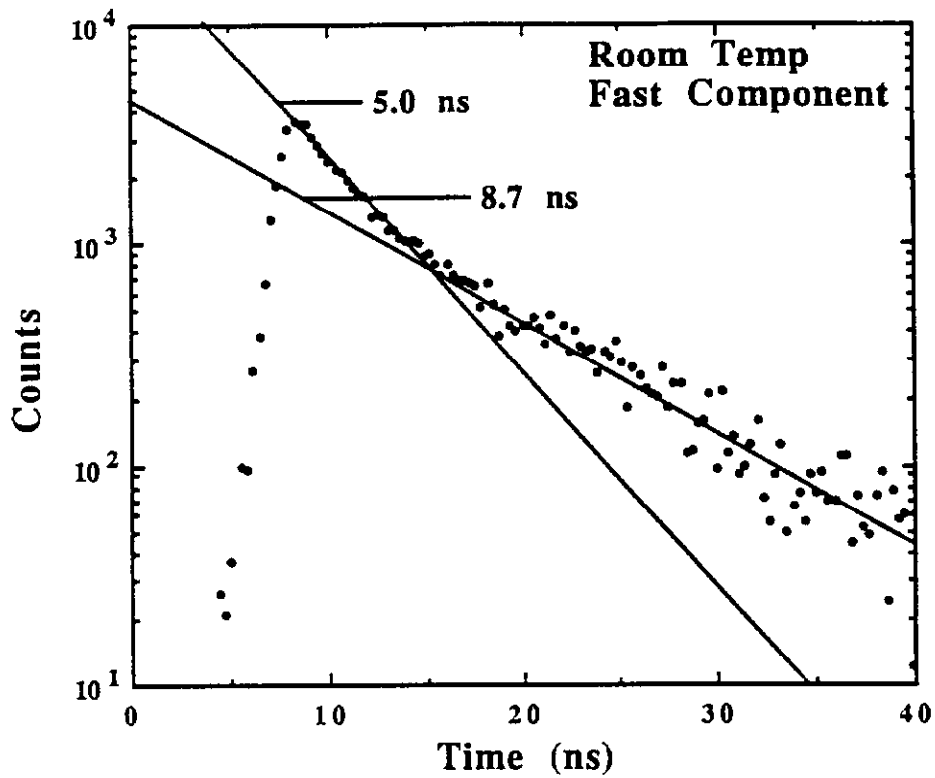


Figure 7 Scintillation decay curve of fast component at room temperature.

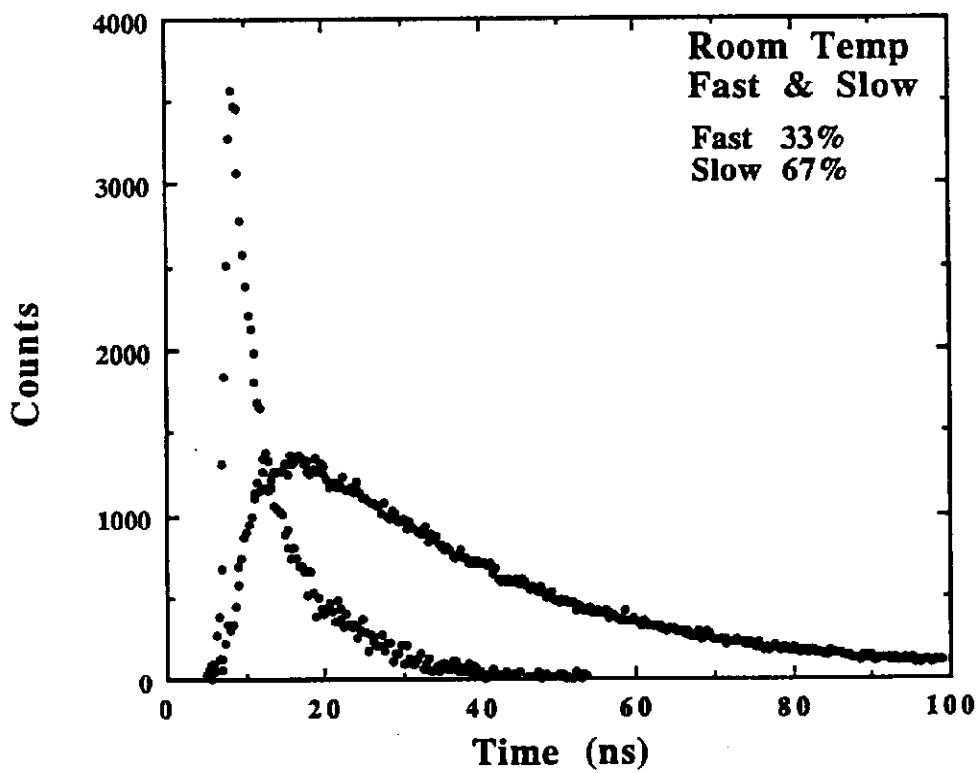


Figure 8 Room temperature scintillation decay curves of fast and slow components on a linear scale.

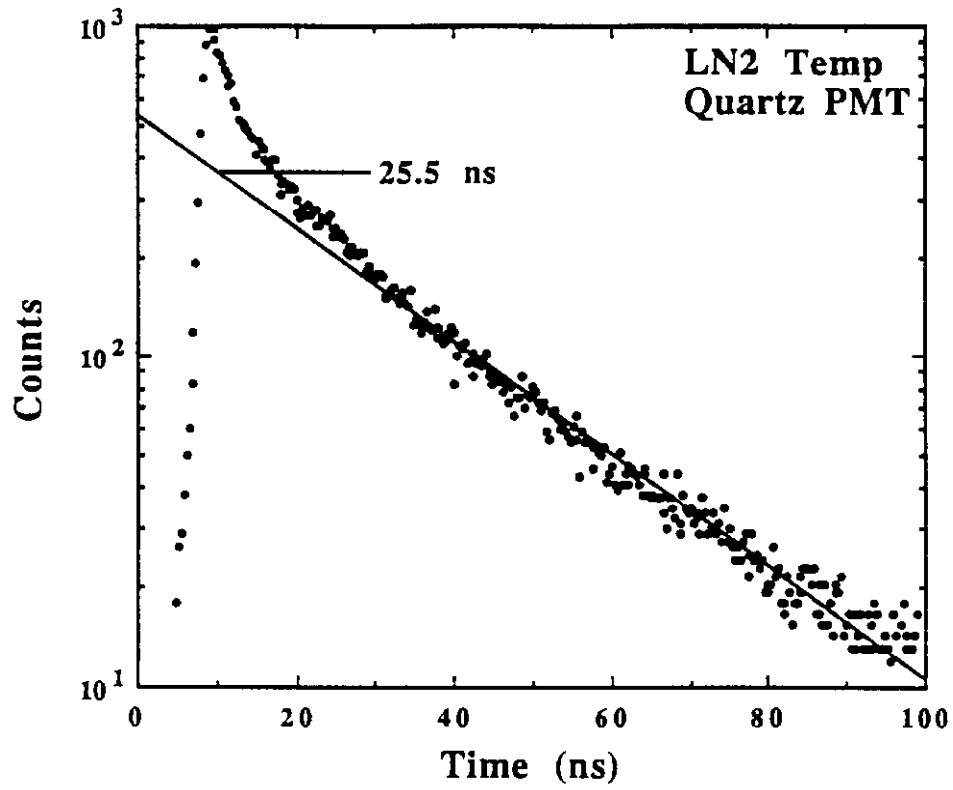


Figure 9 Scintillation decay curve with a quartz PMT at LN₂ temperature .

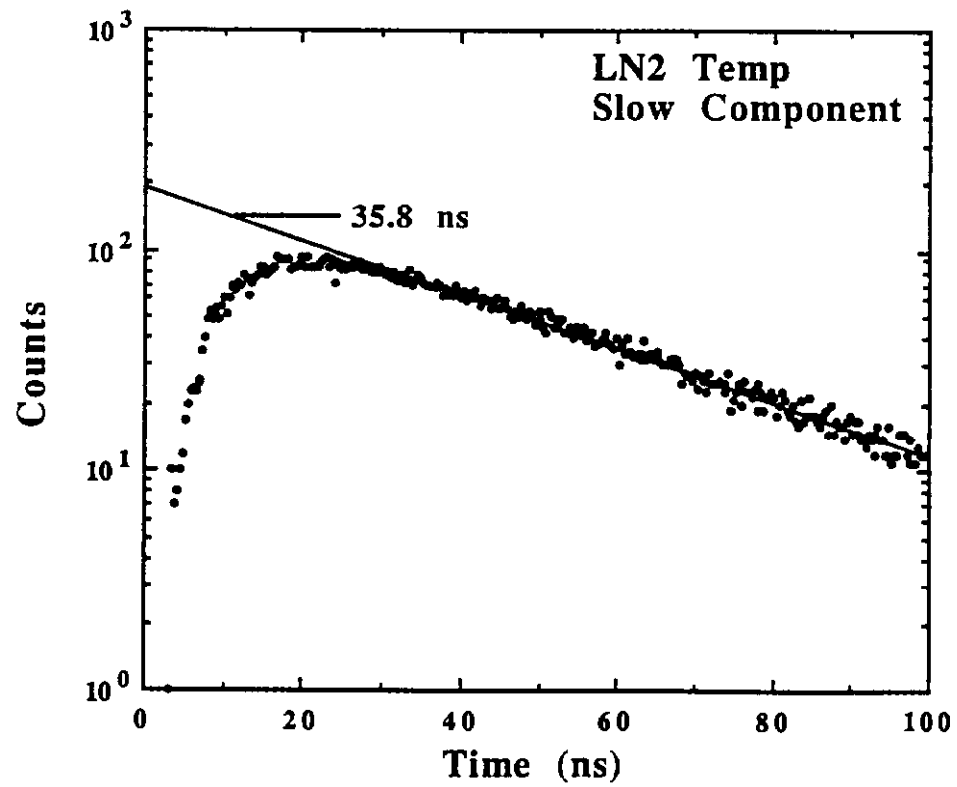


Figure 10 Scintillation decay curve of slow component at LN₂ temperature.

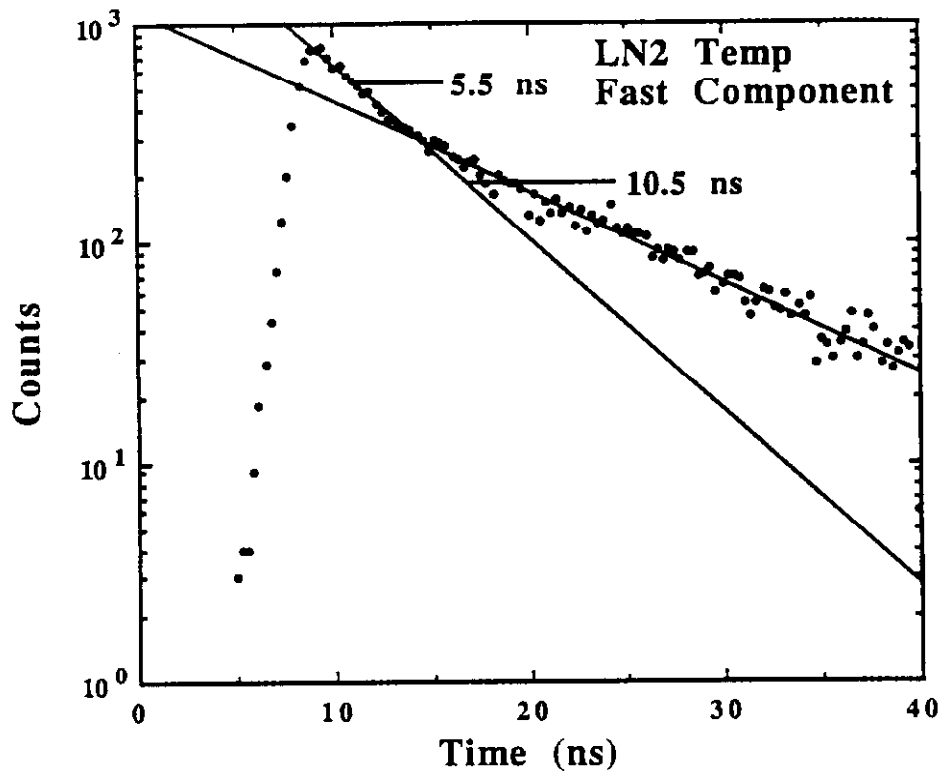


Figure 11 Scintillation decay curve of fast component at LN₂ temperature.

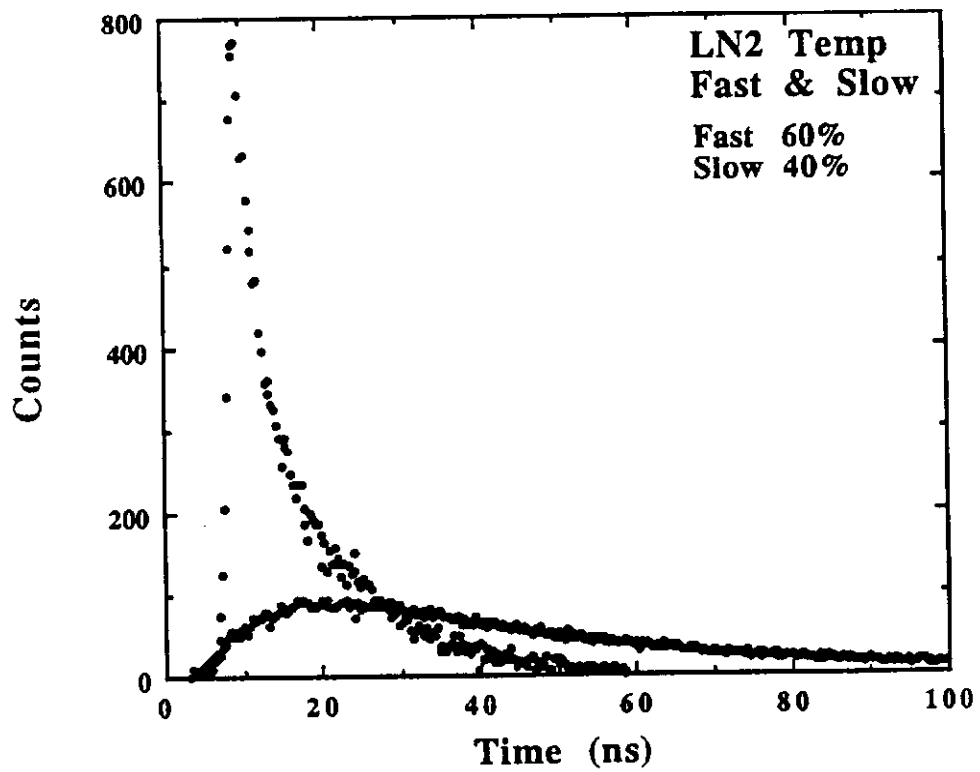


Figure 12 LN₂ temperature scintillation decay curves of fast and slow components on a linear scale.

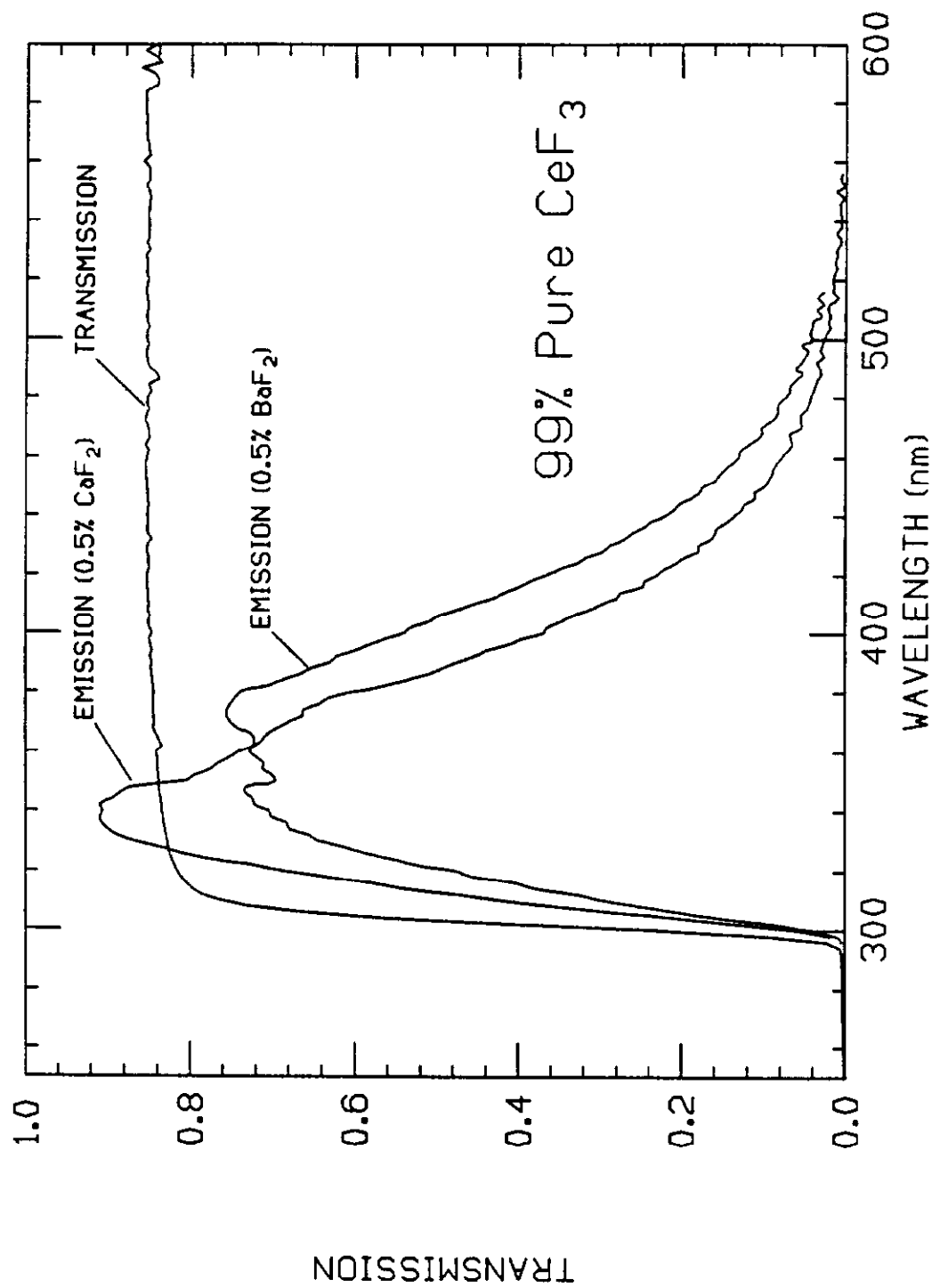


Figure 13 Transmission and emission of 99% pure CeF₃ doped with 0.5% of either CaF₂ or BaF₂. The transmission curves with both dopants are essentially identical.

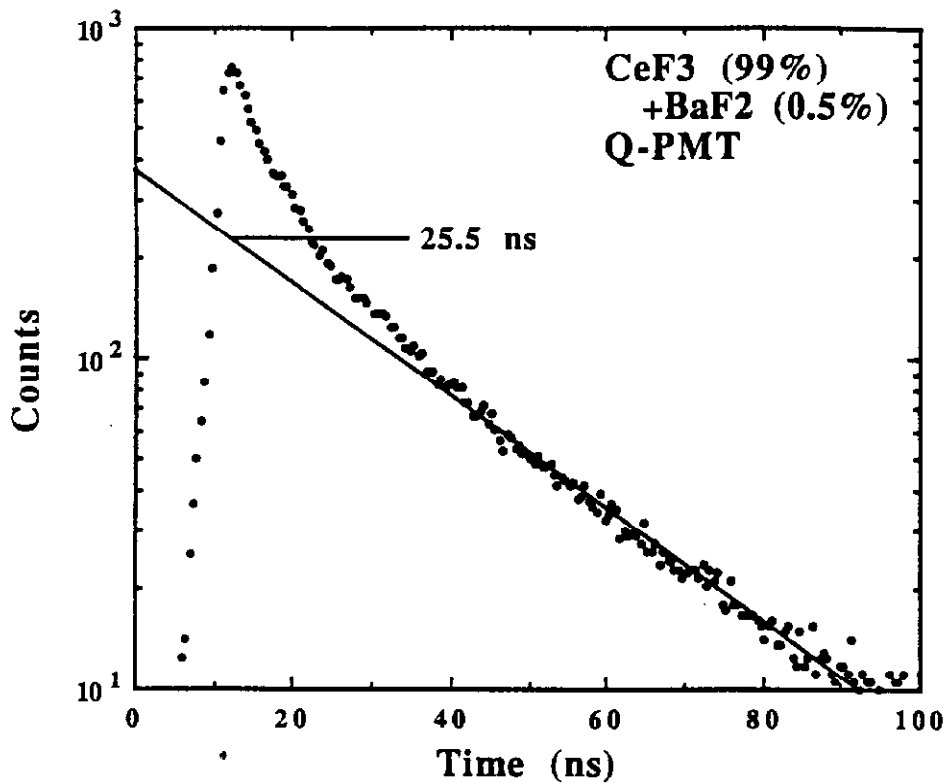


Figure 14 Scintillation decay curve, taken with a quartz PMT, of 99% pure material doped with BaF₂. (Similar results were found for the BaF₂-doped material.)

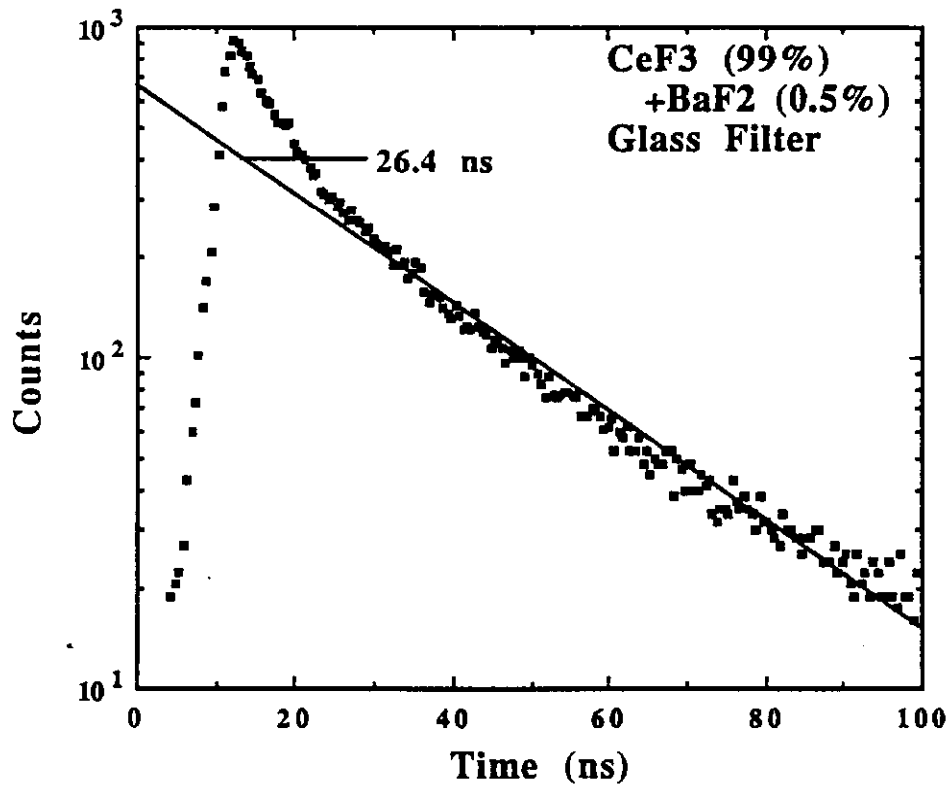


Figure 15 Scintillation decay curve, taken with a glass filter, of 99% pure material doped with BaF₂. (Similar results were found for the BaF₂-doped material.)